TKN **Telecommunication Networks Group**

Technical University Berlin

Telecommunication Networks Group

A Simulation Model for the Performance Evaluation of WirelessHART TDMA Protocol

Osama Khader[*], Andreas Willig[•], and Adam Wolisz[*]

[*] *Telecommunication Networks Group*
Technische Universitat Berlin
Berlin, Germany
Email:khader@tu-berlin.de
Email:awo@ieee.org

[•] *Department of Computer Science and*
Software Engineering
University of Canterbury
Christchurch, New Zealand
Email: andreas.willig@canterbury.ac.nz

Berlin, May 2011

TKN Technical Report TKN-11-001

TKN Technical Reports Series

Editor: Prof. Dr.-Ing. Adam Wolisz

Abstract

Wireless HART is a state-of-the-art solution for a time-division multiple-access (TDMA) based wireless private-area network. It combines slow frequency-hopping and a TDMA scheme that utilizes a centralized a-priori slot allocation mechanism. In this report we conduct a performance evaluation of the WirelessHART TDMA protocol and provide insights into the major factors impacting energy consumption. These insights provide valuable guidance on where to start with any effort geared towards saving energy. The main contributions of this report are: (i) We developed and implemented a simulation model for WirelessHART TDMA protocol. (ii) We conduct a sensitivity analysis of the WirelessHART TDMA energy consumption parameters using the response surface methodology. Based on these results we determine the most influential parameters (transmission, reception, listening, sleeping, turnaround and packet size) for the total energy consumption. (iii) We evaluate and discuss the impact of time synchronization and types of link scheduling algorithms on the performance of WirelessHART TDMA protocol. .

TU BERLIN

Contents

Chapter 1

Introduction

In many application areas of embedded wireless networks, for instance in building automation or industrial control, source nodes send data packets periodically [23], [24], [9] to a gateway or sink node across a set of forwarder nodes. For cost-effective, quick and scalable deployment, sensor nodes often run on batteries and therefore have only a limited amount of energy. The sensed data should be transported reliably and in a timely fashion to the sink. At the same time the operation of the whole network and of individual nodes should be energy-efficient. Therefore, reporting the sensed data reliably while consuming the minimum amount of energy is of great concern. Since the media access layer usually controls the states of the radio, it has a large impact on the overall energy consumption. Different media access methods result in different trade-offs between end-to-end delay and energy-efficiency. From among the large number of existing MAC protocols for wireless sensor networks (e.g. contention-based protocols [6], [20], [28] and contention-free protocols [26], [21], [14]). A TDMA-based protocol has been chosen as a basis for the WirelessHART standard [5]. It is commonly thought that TDMA-based protocols offer good opportunities for energy-efficient operation of sensor nodes, as they allow nodes to enter sleep mode when they are not involved in any communications. Furthermore, TDMA is the method of choice for applications in industrial and process automation (and many other application areas), since it offers a level of determinism that is not achievable with other types of MAC protocols. WirelessHART utilizes the physical layer of IEEE 802.15.4 and specifies a new MAC protocol. This new MAC protocol combines frequency hopping with a TDMA scheme utilizing a centralized a-priori slot allocation mechanism. WirelessHART forms mesh topology network and all the devices must have a routing capabilities. The goal of this report is to evaluate the WirelessHART TDMA protocol in terms of the overall energy consumption of the different types of nodes (sources and forwarders). However, we go beyond mere reporting of energy consumption figures for various deployment scenarios. Specifically, we analyze how the overall energy consumption breaks down into different factors. By identifying the factors contributing most to the overall network energy consumption, we can provide guidance on where to start with any effort geared towards saving energy. On the other hand, several communication standards such as ZigBee [2] and ISA [1] have been applied in the industrial automation fields. Most of the energy consumption models proposed in the literature are based on the ZigBee standard that uses CSMA/CA MAC (IEEE 802.15.4 MAC). In ZigBee there is no frequency diversity and the entire network operates in the same static channel. Also there is no path diversity as a new

TKN-11-001   Page 3

path from source to destination has to be set up whenever the link is broken. This increases both delay and overhead and leads to an increase in energy consumption. Therefore, energy consumption models proposed for ZigBee can not be applied to WirelessHART. A separate performance evaluation of energy consumption of the WirelessHART is essential. Our main contributions can be summarized as follows:

1. We developed a simulation model for the WirelessHART TDMA protocol using Castalia and OMNeT++ simulation frameworks [27], [19].

2. We performed a sensitivity analysis of the WirelessHART energy consumption parameters using response surface methodology. We determine the most influential parameters for the total energy consumption among the following factors: transmission, reception, listening, sleeping, turnaround and packet size.

3. We evaluated and discussed the impact of synchronization and type of link scheduling algorithms on the performance of WirelessHART TDMA protocol.

To the best of our knowledge, this report provides the first detailed analysis of the main factors contributing to the energy consumption of WirelessHART.

The remainder of the report is structured as follows. Chapter 2 presents an overview of the WirelessHART standard. Chapter 3 explains the network manager design components used in this report. Subsequently Chapter 4 describes the simulation-based performance evaluation approach used in this report. The sensitivity analysis and the results are presented in Chapter 5. Here we also present results for the impact of time synchronization on the performance of the WirelessHART TDMA protocol. Related work is presented in Chapter 6 and finally, Chapter 7 concludes the report with some possible ideas for future work.

TKN-11-001   Page 4

Chapter 2

Overview on Wireless HART

WirelessHART [10], [12], [11], [13] (abbreviated as WHART in the following) is one of the first wireless communication standards specifically designed for process automation applications. The standard has been finalized in 2007, and at the beginning of 2010 it has been ratified as an IEC standard. On the physical layer, WHART adopts radios that are compliant to the IEEE 802.15.4 standard [15]. It operates in the 2.4 GHz band and offers a bit rate of 250 kbit/s. On top of the physical layer, WHART employs a TDMA-based MAC protocol and additionally performs slow frequency hopping (hopping on a per-packet basis). The frequency hopping-pattern is determined from a well-known pseudo-random sequence. The TDMA slot allocation is centrally controlled and slots are assigned at network configuration time.
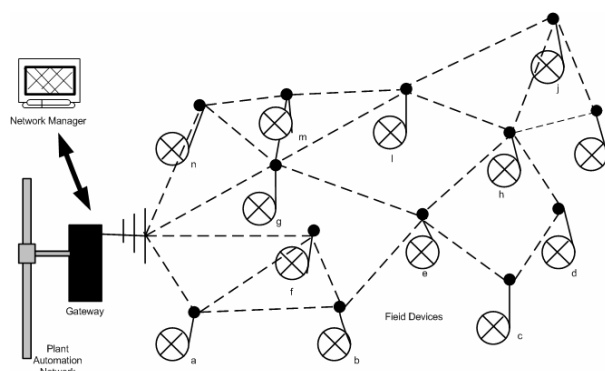

Figure 2.1: WirelessHART basic network components

2.1 Network architecture

The network architecture of a WHART network features three different types of components (compare Figure 2.1).

TKN-11-001
Page 5

2.1.1 Field device

The WHART **field devices** are used for collecting measurement data from the field and for forwarding this data to a gateway node. They typically integrate wireless communication, sensing, and computational facilities. A field device might be either a genuine WHART device or it might be a legacy (wired) HART device equipped with a HART-specific wired-to-wireless adapter. In this report we assume that field devices are battery-driven, so we are especially interested in their energy-consumption.

2.1.2 Gateway

A **gateway** forms the boundary between a WHART segment and other (often wired) parts of an automation network and is not energy-constrained. The gateway is the point where all sensor data provided by WHART field devices is collected and prepared for further processing. It enables communication between host applications and field devices. There is only one gateway per network and all the WHART devices are known to the gateway.

2.1.3 Network manager

The **network manager** is a centralized unit. It has global information about the network topology, link qualities and the traffic flows. Based on that, it computes a routing and a TDMA schedule and disseminates it to the remaining participants. Slots in the TDMA schedule are allocated hop by hop based, all other stations are allowed to sleep during a slot. The network manager not only allocates slots, but places those slots also on different frequencies. The network manager has further responsibilities, including the monitoring and health reporting of the WHART network and adapting the network to ongoing changes. The network manager is not assumed to be energy-constrained.

2.2 The WirelessHART TDMA Scheme

In this section, we briefly discuss the WHART TDMA scheme. The timing hierarchy of WHART has three levels. On the lowest level we have individual **time slots**. Within one time slot one data packet and the accompanying immediate acknowledgement packet are exchanged. A time slot in WHART has a fixed length of 10 ms. A contiguous group of time slots of fixed length forms a **superframe**. On top of that, a contiguous group of superframes forms a **network cycle**. Within each cycle each field device receives at least one time slot for data transmission, but certain devices may have more time slots than other devices because they have more data to report or they have additional forwarding duties.

An individual field device receives a schedule from the network manager informing him about those time slots where it transmits and those slots where it receives. Furthermore, a field device must maintain time synchronization to agree on slot boundaries with neighbored devices.

2.3   Dedicated time slots and Time Synchronization

In WHART two types of time slots are available: dedicated time slots and shared time slots. Here we consider only dedicated time slots, which are allocated to one specific sender-receiver pair.

The internal structure of a dedicated slot is displayed in Figure 2.2.
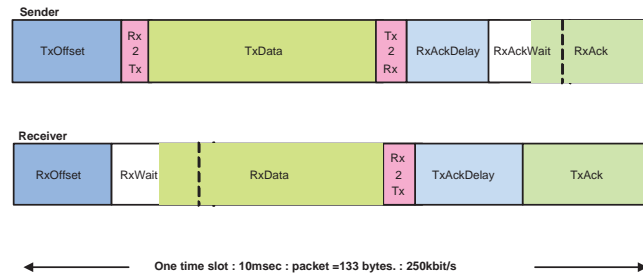

Figure 2.2: Dedicated slot timing

We first discuss the operation of the receiver node. It enters the receive state at the beginning of its time slot. The receiver measures the exact time when it has detected the start of the packet sent by the transmitter. The expected time for this to happen is `TxOffset`.seconds after the start of the slot. The receiver computes the difference / timing offset between the actual time when it detects the start of the packet and the expected time. When the receiver has successfully received the packet it turns his transceiver into transmit mode, sends an acknowledgement packet, and returns into receive mode. This acknowledgement includes the measured offset and allows the transmitter to adjust his local time accordingly.

The transmitter also starts a time slot with its transceiver being in receive mode. After time `TxTxOffset` it turns the transceiver into transmit mode, sends the data packet, turns into receive mode and waits for the acknowledgement. The measured offset contained in the acknowledgement is used by the transmitter to re-calculate its local view on the start times of time slots.

This approach to clock readjustment is the elementary building block for WHARTs overall time synchronization scheme. In general, due to the fact that hardware clocks are imprecise, time synchronization in multi-hop system is a problem [7], [8]. There are two main factors affecting accuracy of local time. The first is clock drift, which indicates the rate at which a clocks actual frequency deviates from its nominal frequency; and the second is clock offset, which is the difference from ideal time. For proper operation of the TDMA algorithm neighboring nodes need to agree on boundaries of time slots and therefore a clock synchronization algorithm is needed. WirelessHART uses the above-described device-to-device adjustment method for this purpose. In addition, each device sends a keep-alive packet periodically (each 60s) to combat clock drifts. A synchronization tree is built with the gateway at its root. Essentially, devices at depth d in the tree synchronize their clocks to devices at depth $d-1$. The gateway has depth 0, its immediate neighbors have depth 1 and so on.

For example, if a node scheduled to receive a packet, it starts listening for RxOffset time from the start of its slot. After the arrival of the first bit of the packet the node

must acknowledge a packet within MaxPacket + TxAckDelay time unites. The size of the acknowledge packet is 26 bytes and it carries 2 bytes time adjustment field measured in microsecond to be used in the time synchronization process.

The state diagram for the WirelessHART TDMA protocol is shown in figure 2.3. The TDMA machine specifies the overall operation, mainly link schedules, and maintaining the time synchronization.
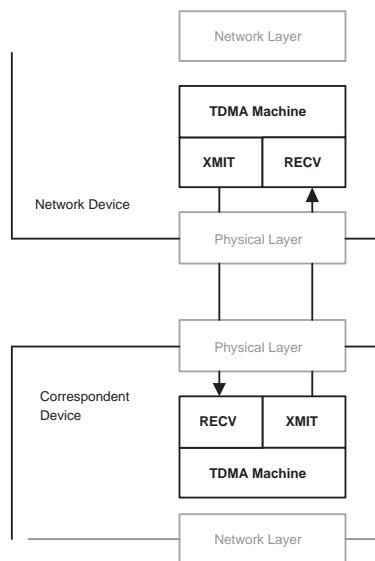
Figure 2.3: WirelessHART TDMA MAC components

The transmitter engine (XMIT) is responsible for sending packets to the corresponding node. The receiver engine (RECV) performs listening and receives an incoming packet. These two aspects are discussed next.

2.4 XMIT engine

When a transmit slot starts, the device enters *Talk* state by invoking the XMIT engine and transmits the packet. If the packet transmission fails then the device will try to retransmit in the pre-assigned retransmission slots for this device.

Upon successful transmission and if the packet destination field is not broadcast, the TDMA machine enters the *wait for ACK* state by initializing the RxDelay timer to RxAckDelay and the receive window (RxWindow) to AckWait and invoking the RECV engine. When a packet is to be transmitted, the XMIT engine is called to perform the actual packet transmission.

2.5   RECV engine

The receive path is managed by the RECV engine. This engine is invoked to acquire a data or ACK packet that is being sent by one of the neighbors. When the RECV engine is invoked, the transceiver is configured by selecting the correct channel. In addition, the RxDelay timer is started and the *Wait For Rx Start* state is entered. During the RxDelay the transceiver is allowed to settle and synchronize to the correct channel. The *Wait for Rx Start* state is left when the RxDelay timer expires.

The RxDelay timer is set by the TDMA machine to allow the receiver to become active at the beginning of the receive window. The duration of the receive window is controlled by the RxWait timer which is started after the RxDelay timer expires. The node remains in the *Listen for Packet* state until either 1) the start of a packet is detected or 2) the Rx timer expires and an RxTimeout occurs. If there is no addressing error, the received packet is validated, otherwise the RECV engine terminated indicating "No response".

Chapter 3

Network Manager Design

The network manager is a centralized unit having global information about network topology, link qualities and traffic demands. It is responsible for the overall network operations. Please note that for whatever purposes, the WHART standard leaves many details open. For example, the standard does not fully define or introduce a TDMA slot allocation algorithm, it just provides some constraints that any such algorithm has to obey. For the purposes of this study we design and implemented an instance of the network manager that performs the two main functionalities of computing the link scheduling and the paths. The following sections describe the the core network manager functionalities that we consider in our simulation model.[1]

3.1   Core network manager components

Figure 3.1 illustrates the core network manager components. Each node on the WHART network has to send its information (node ID and neighbor table) and its communication requirements (traffic rate, priority). Thus the network manager has a complete list of all the nodes and the overall network topology. The network manager then computes the routes and assigns slots based on the information received from each node. This include superframe table which contains frameID, number of slots and channels list. The link table which includes, nodeID, slot number, link option (Tx, Rx), link type (unicast, broadcast, join, discovery). The routing table includes the routeID and destination address. For scheduling algorithm we implemented two main scheduling algorithms, breadth-first scheduling and depth-first scheduling. For routing we used multi-path routing [18]. These two aspects are discussed next.

3.2   Link scheduling

One of the main tasks in designing a TDMA protocol is the allocation of time slots to sender-receiver pairs. Determining a throughput-optimal schedule for TDMA slot assignment in multi-hop network is NP-complete even in linear networks [3]. Some of the constraints that scheduling algorithms have to follow in WHART are:

---

[1]Please note that the security manager of WHART is not considered in our study.

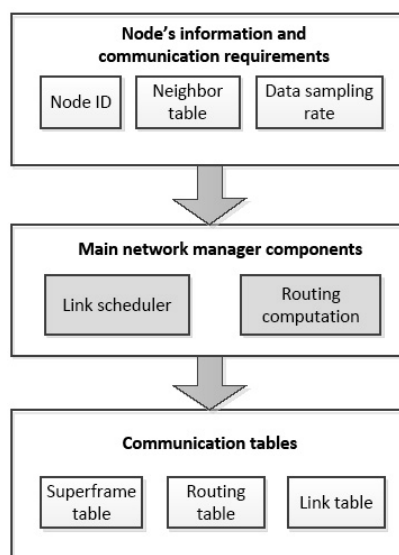TKN-11-001   Page 10

Figure 3.1: Core network manager components

1. Management slots have priority over data slots.

2. Each device gets three slots every 15 minutes for health reports.

3. Each device gets at least one slot every minute for management packets (advertisement, join request/response, command request/response).

4. Each device gets a slot for keep-alive packets every 60 seconds.

5. Slots for stations having the fastest transmission periods are allocated first.

6. Allocate at least one backup slot to each data slot to handle a retry.

Since WHART does not support the spatial reuse of time slots in the same channel[2], we do not consider it.

3.3 Breadth-first approach

Figure 3.2 shows an example of the breadth-first approach. The network manager assigns time slots starting from the outmost sources. In the example, nodes S1, S2, and S3 are the sources, whereas nodes F1, F2, and F3 are the forwarders. The Network manager assigns one data slot for each source. For the first forwarder F1 it assigns one slot to forward the data of S1. F2 has two slots to
forward the data for S2 and S3. F3 has three slots to forward the data it receives from F1 and F2. According to the breadth-first approach, time slots 1, 2 and 3 are assigned to sources

---

[2]WHART supports parallel transmission on different channels only.
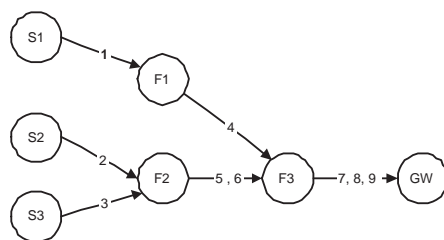
Figure 3.2: Example of breadth based approach

S1, S2 and S3, respectively. Slot 4 is assigned to forwarder F1, slots 5 and 6 to forwarder F2, and slots 7, 8, and 9 to forwarder F3.

The time-slot assignment in the breadth-first approach is organized so that sources get the first slots, followed by the forwarders directly attached to sources (first-wave forwarders), followed by forwarders directly attached to first-wave forwarders and so on. This might cause a buffer problem for the later forwarders, since such a forwarder has to buffer all packets from forwarders from previous waves before getting a chance to empty his own buffer. In our example, it might happen that forwarder F3 has only two packet buffers. This would result in frequent buffer overflow.

3.4 Depth-first approach

The network manager applies the depth-first approach as shown in Figure 3.3. S1 generates a packet in time slot 1, time slot 2 is assigned to F1 to forward the received packet to F3,
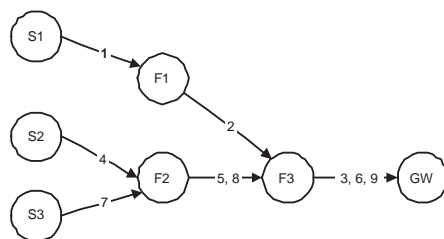
Figure 3.3: Example of depth based approach

time slot 3 assigned to F3 for forwarding the packet to the GW. S2 generates its packet in time slot 4, time slot 5 is assigned to F2 and time slot 6 to F3. Similarly, S3 assigned time slot 7, time slots 8 and 9 are assigned to F2 and F3, respectively.

This assignment method avoids buffer overflows in forwarders.

3.5 Route Computation

Based on the link information provided by each node, the network manager creates the so called routing graphs, i.e. the collection of all vectors that join source and gateway of each link. In this process, the network manager follows several rules based on the standard: (i) Minimize the number of hops. (ii) Route through powered devices if they are available. (iii) Use signal strength to select the best paths to neighbors. (iv) Use a combination of weighted signal strengths to select between alternative routes.

Alternatively, the network manager can also be configured to use traditional address routing (source routing).

TKN-11-001   Page 13

Chapter 4

Performance Evaluation Approach

In this chapter, we describe our approach for evaluating the performance of the WHART TDMA protocol in terms of energy, consumed in the overall network. Please note that the energy consumption is calculated only for the source and forwarder nodes. We do not take into account the gateway energy consumption in our calculation as its assumed to be directly connected to a power source.

4.1   Simulation setup

In order to realize a simulation model to study the performance of WirelessHART TDMA over a wireless multi-hop network, we have chosen the OMNeT++ [27] simulation environment together with the Castalia framework [19]. OMNet++ is an open-source discrete-event simulator, Castalia is an OMNet++ based framework designed specifically for wireless sensor networks. We set the radio parameters based on the IEEE 802.15.4-compliant ChipCon CC2420 radio chip [4]. The CC2420 operates in the 2.4 GHz ISM band and supports eight transmission power settings in the range between -25 dBm and 0 dBm. For the wireless channel we use the log-normal shadowing model which has shown to give an accurate estimates for average path loss[16] . Generally speaking the path loss PL is a function of the distance d from the transmitter as shown in the following equation:

$$PL(d) = PL(d_0) + 10.\eta.Log\left(\frac{d}{d_0}\right) + X_\sigma \tag{4.1}$$

$PL(d)$ is the path loss at distance d, $PL(d_0)$ is the known path loss at a reference distance d_0, η is the path loss exponent, and X_σ is a Gaussian zero-mean random variable with standard deviation σ. For the channel fading model we used the Rayleigh fading model. Generally speaking, for stationary sensor nodes and low sampling rates deployed in fairly static environments (not large moving objects), Rayleigh fading model is fairly reasonable and most commonly used. In the channel model when calculating the path loss at a specific instance of time, we first find the average path loss from the state we have stored during the channel initialization and then find the component of the path loss due to channel fading. In order to achieve this we have to keep the last observed vale which in reality the last value we computed and the time it has passed since then. These two values define a probability density

Table 4.1: Power consumption of CC2420 radio with 3.3 V supply voltage

Main power consumption of CC2420 radio			
Notation	Parameters	I(mA)	Power(mW)
P_{Tx}	Transmit power (0dBm)	17.4	57.42
P_{Rx}	Receive power	18.8	62.04
P_L	Listen power	18.8	62.04
P_S	Sleep power	0.426	1.406

function that we draw our new value from. Thus, the probability density function returns bigger values if the last observation in a deep fade (e.g -40dB), otherwise it returns close value to the last observation one. The values of the channel parameters are listed in Table 4.2. For channel errors we use the Castalia's realistic channel model with its random packet loss. That is, the simulator calculates for every link a packet reception rate PRR, which represents the probability that a packet is successfully transmitted. With these random link qualities, we choose to use only links having a PRR¿ 0.9. For more detailed information about the derivation of these values, please refer to the Castalia's user manual [19]

For our implementation of the WirelessHART TDMA we created a list of channels for the simulation to switch between following the pseudo-random sequence. As our report focuses on energy consumption we assume that, all the channel have identical behavior. We modeled the cost of channel switching. Channel switching is modeled in both receiving and transmission slots within the TxOffset and RxOffset time intervals, respectively. The transceiver has four main operational states: transmit, receive, listen and sleep. Given that for long-running applications most of the energy will be spent in the operational phase of a MAC protocol, we have chosen to ignore the initialization phase in the simulator. The TDMA schedule is pre-computed based on the breadth-firs and depth-first scheduling algorithms and given as input to the simulator.

In Table 4.1 the main power consumption parameters of a CC2420 transceiver are summarized assuming a 3.3V supply voltage. These parameters are used in the physical layer model of our simulator to obtain energy-consumption results. The simulation records the amount of time spent in various states (transmit, receive, listen and sleep). We also model the energy spent in switching between states by multiplying the turnover time by the power consumed in the most power-consuming of the two involved states. At the end of each run, the simulation computes the total energy consumed for each node in the network using the amount of energy consumed by the radio in each state (thus ignoring the node's microcontroller).

Further simulation parameters related to the physical and MAC layer properties and the node deployment are given in Tables 4.2 and 4.3, respectively. When the nodes are powered on, they are all unsynchronized. In order to achieve synchronization among the nodes, the gateway will take initiative to start controlling a time slot. All the nodes will synchronize their clocks to the gateway. We have conducted a variety of scenarios in our evaluation, including a single-flow, multiple-flows, and random scenarios. We also conducted simulation under different traffic rates and link scheduling algorithms. These are discussed next.

Table 4.2: General parameters

Main Radio and MAC parameters	
Notation	Parameters
Radio layer	CC2420
Data rate	250kbps
Packet size	133
$PL(d_0)$	54.2dB
η	2.4
X_σ	4.0
Number of slots per superframe	100s
Slot-time length	10ms
Synchronization packet size	26 bytes
Resynchronization rate	60s
Health report rate	15min

4.2 Single-flow scenario

A schematic of our first scenario is shown in Figure 4.1. We assume a single source, 12 forwarders, and one gateway. The forwarder nodes are arranged in grid topology. The distance between the source node and each of the forwarding nodes to which the source node is directly connected is within the range of 10 to 12m. The sink node connected to the last forwarding nodes as depicted in the figure has the same distance as between the source and the forwarding nodes.
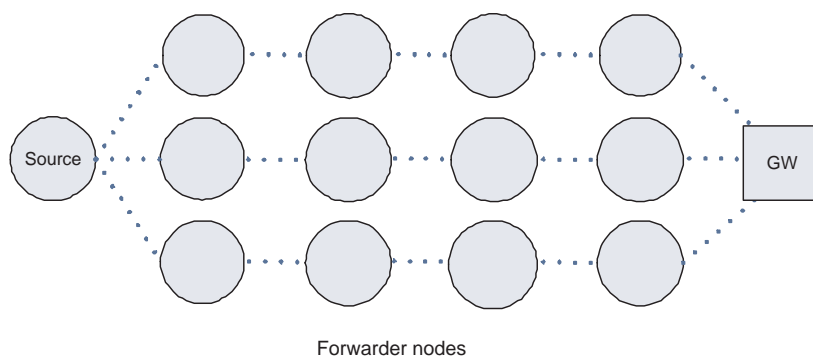

Figure 4.1: Single source scenario

The source periodically generates packets up to 133 bytes in total size, The generation period was varied, ranging from 1 to 30 to 60 seconds. Within one run we generate 5000 packets. MAC-layer acknowledgments are enabled and the size of the ACK packet is 26
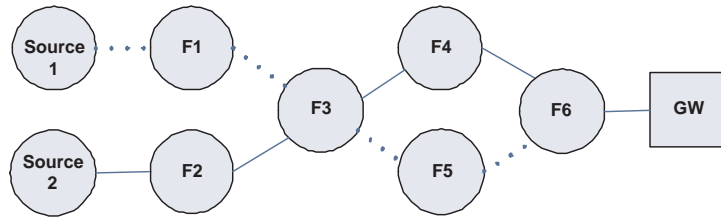
Figure 4.2: Multiple source scenario

bytes. If the packet is lost due to channel errors the sender tries to transmit the packet for a maximum of two retries. We apply multi-path routing [18], i.e. in the setup phase the source is configured with a set of possible paths and then randomly selects a single path out of a set of given paths.

4.3 Multiple-flow scenario

The multiple-flow scenario includes two sources, five forwarders and a single gateway (see Figure 4.2). Similar to the single-flow scenario each source node periodically generates packets of 133 bytes size. The distance between any two adjacent nodes is 10m. The second hop (F3) shares two flows. The remaining configuration is identical to the single-flow scenario.

4.4 Random scenario

To test if our analysis independent of the underlying network topology, we generate 100 random topologies and take the average as a final result. 150 nodes are deployed randomly (uniformly distributed) over a 120m x 120m. Three to five nodes are randomly picked up as source nodes. Each of the sources sends 5000 packets to the GW via some forwarder nodes. As shown in Figure 4.3 the GW is placed in the top right corner of the figure. The sources chosen such that the path length is 4 to 12 hops. Any path less than 3 hops is discarded and not considered in the evaluation. The remaining configuration is identical to the previous scenarios.

4.5 Sensitivity analysis

The major goal of our study is not only to obtain insights into the overall network energy consumption of the different types of nodes (sources and forwarders) in the considered network deployments, but we also want to obtain some insights on how the overall consumption breaks down into different factors. By identifying the factors contributing most to the overall network energy consumption, we can provide guidance on where to start with any effort geared towards saving energy.

Our major tool for achieving this is the Response Surface Methodology (RSM). RSM is a collection of mathematical and statistical techniques useful for modeling and analysis of problems in which a response of interest is influenced by several variables and the objective is
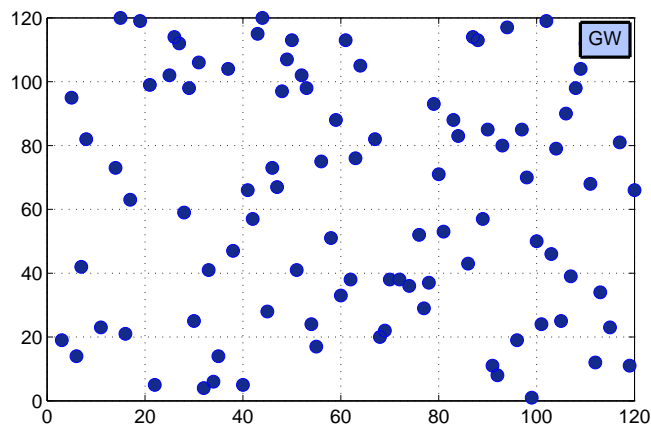
Figure 4.3: Example of a random scenario

Table 4.3: WirelessHART TDMA MAC parameters

Notaion	Parameters	value (ms)
WirelessHART MAC parameters		
TxOffset	The guard time at beginning of time slot at the sender side.	2.12
RxOffset	The guard time at beginning of time slot at the receiver side.	1.12
RxWait	The time to wait for start of packet	2.2
MaxPacket	Maximum packet length	4.256
TxAckDelay	The time between end of packet and start of ACK at the receiver side.	0.8
RxAckDelay	The time between end of packet and start of listening for ACK at the sender side.	0.9
AckWait	The minimum time to wait for start of an ACK	0.4
Ack	ACK (26 bytes)	0.832
RxTx	TxRx turnaround time	0.192

TKN-11-001
Page 18

to optimize the response. Basically, a linear model is identified which explains the response in terms of individual factors and combinations factors:

$$Y = \beta_0 + \sum_{i=1}^{k} \beta_i x_i + \epsilon \qquad (4.2)$$

If there is curvature in the system, then a polynomial of higher degree must be used, such as the second order model:

$$Y = \beta_0 + \sum_{i=1}^{k} \beta_i x_i + \sum_{i=1}^{k} \beta_{ii} x_i^2 + \sum_{i<j} \sum \beta_{ij} x_i x_j + \epsilon$$
$$For \, i = 1, 2, ..., k, and \, j = 1, 2, ..., k. \qquad (4.3)$$

Where Y is the response variable, $x_1, x_2, \ldots, x_k$ are the input factors, k is the number of factors, β_0 is the intercept term and β_i are the regression coefficients. ϵ is the random error which is assumed to be distributed as a normal distribution with zero mean and unknown variance. The method of least squares can be used to estimate the parameters in the approximating polynomials. The response surface analysis is then performed using the fitted surface. If the fitted surface is an adequate approximation of the true response function , then analysis of the fitted surface will be approximately equivalent to analysis of the actual system. Furthermore the method of steepest descent is a procedure for moving sequentially in the direction of the minimum decrease in the response. If maximization is desired, then we call this technique the method of steepest ascent. The direction and step size in which the factors are varied to improve the measure response are determined using the sign and regression coefficient. The relationship between the response variables and the identified factors usually represented graphically by a so-called three-dimension response surface graph. Additionally, it is helpful to plot the counter plot which visualize the shape of the response surface. We will see such graphs later in our results. For more details about the RSM we point the reader to the [22] and also see [17].

4.6   Factor screening

The first step in the RSM is to identify potential factors affecting the response being measured (factor screening). Since the total energy consumption for the overall network (sources and forwarders) is the main response, we consider the following factors:

- Factor A – Transmission energy: the transmission energy is the energy consumed for transmitting data packets and control packets such as synchronization packets.

- Factor B – Receiving energy: the receiving energy is the energy consumed while receiving data and control packets.

- Factor C – Listening energy: we define the listening energy as the radio energy consumption when the radio is on but not receiving or sending any packets.

Table 4.4: The factors and the levels of each factor

Term	Factor	Level 1(-1)	Level 2(+1)
A	Tx power	32.67mW	57.42mW
B	Rx power	31.68mW	62.04mW
C	Listen power	31.68mW	62.04mW
D	Sleep power	0.72mW	1.41mW
E	Turnaround power	31mW	62mW
F	Packet size	26 bytes	133 bytes

- Factor D – Sleeping energy: the sleeping energy is the energy consumption while the radio is in the low-power state.

- Factor E – Turnaround energy: the turnaround energy is the energy consumed for switching the radio state between different modes.

- Factor F – Packet size: The energy consumed for transmitting or receiving a full packet to the wireless channel.

Table 4.4 lists the factors and the levels of each factor considered in our study in case of no channel errors and with channel errors. The levels of the factors are based on the WHART specification and the data sheet of the CC2420 radio model. Given the five factors of interest, we perform a 2^6-factorial screening experiment to identify the percentage contributions of each factor. Each simulation result was averaged over 10 runs for each factor. Since we have 2^6 factors, we performed a total of 640 simulation runs for factorial screening for each scenario with channel errors and without channel errors, respectively.

Chapter 5

Analysis of the results

In this chapter, we analyze and determine the most influential parameters for the total energy consumption. We also provide results demonstrating the impact of the time synchronization on the performance of WirelessHART TDMA protocol across various scenarios.

5.1 Results in case of single-flow scenario

Tables 5.1 and 5.2 show the percentage of the individual factors and their pairwise combinations contribute to the total energy consumption in case of no channel errors and with channel errors, respectively.

From the statistical analysis it can be seen that factor C (sleep power) and D (Listen power) contribute most to the total energy consumption in both cases. To get more statistical details of the factors affecting the total energy consumption, we perform an analysis of variance (ANOVA) as shown in Tables 5.3 and 5.4.

The ANOVA shows the effect of each design factor on the total energy consumption and their statistical significance through the F-test and associated probability ($Prob > F$). F-value column reports the ratio of the mean squares of the model over the mean squares of the residual. The F-value is compared to the reference distribution for F, in order to determine the probability of observing this result due to error. If the value in the last column of the table is less than 0.05 (95 percent significance level), then the factor is statistically significant. In other words, there is a very small probability, near 0.01% that the differences in the factors model averages are due to the chance variation.

The results given in Table 5.3 demonstrates that all the elementary and the compound factors (AF, BF, CF) are highly significant, together they explain almost all the variation. For channel error scenario, Table 5.4 demonstrates that all of the elementary and the compound factors are highly significant.

Moreover, the ANOVA Tables in both cases (with channel errors and without channel errors) show the goodness of the regression using the coefficient of determination R^2 [1] which gives the proportion of total variation of the response explained by the model (computed as the ratio of the sum of squares (SSR) to the total sum of squares (SST)).

---

[1]A higher R^2 value, the better the regression.

TKN-11-001   Page 21

Table 5.1: The percentage of factors contribution in case of no channel errors

Term	Sum of Squares	Percentage contribution
A	296.266	1.043
B	336.88	1.186
C	**9118.09**	**32.099**
D	**18186.6**	**64.025**
E	10.997	0.039
F	1.432	$5.042 \cdot 10^{-3}$
AF	66.543	0.234
BF	64.079	0.225
CF	324.433	1.142
Error	$3.397 \cdot 10^{-6}$	

Table 5.2: The percentage of factors contribution in case of channel errors

Term	Sum of Squares	Percentage contribution
A	948.249	2.764
B	133.294	0.388
C	**14265.1**	**41.588**
D	**18109.3**	**52.795**
E	10.869	0.033
F	29.973	0.087
AB	46.158	0.135
AC	548.397	1.600
AD	0.076	$2.215 \cdot 10^{-4}$
AE	$5.653 \cdot 10^{-4}$	$1.648 \cdot 10^{-6}$
AF	0.45	$1.308 \cdot 10^{-3}$
BF	17.94	0.052
CF	121.62	0.35
DF	$1.156 \cdot 10^{-4}$	$3.369 \cdot 10^{-7}$
EF	$3.511 \cdot 10^{-5}$	$1.023 \cdot 10^{-7}$
ABF	14.987	0.044
ACF	54.78	0.160
Error	$3.198 \cdot 10^{-4}$	

Table 5.3: ANOVA for total energy consumption in case of no channel errors

Source	Degree of freedom	Sum of squares	Mean Square	F-value	Prob > F value
Model	9	28405.34	3156.15	$5.017 \cdot 10^{10}$	0.0001
A	1	296.27	296.27	$4.709 \cdot 10^{9}$	0.0001
B	1	336.88	336.88	$5.355 \cdot 10^{9}$	0.0001
C	1	9118.09	9118.09	$1.449 \cdot 10^{11}$	0.0001
D	1	18186.62	18186.62	$2.891 \cdot 10^{11}$	0.0001
E	1	11.00	11.00	$1.748 \cdot 10^{8}$	0.0001
F	1	1.43	1.43	$2.277 \cdot 10^{7}$	0.0001
AF	1	66.54	66.54	$1.058 \cdot 10^{9}$	0.0001
BF	1	64.08	64.08	$1.019 \cdot 10^{9}$	0.0001
CF	1	324.43	324.43	$5.157 \cdot 10^{9}$	0.0001
Error	54	$3.397 \cdot 10^{-6}$	$6.291 \cdot 10^{-8}$		
$R^2 = 0.99$					

Table 5.4: ANOVA for total energy consumption in case of channel errors

Source	Degree of freedom	Sum of squares	Mean Square	F-value	Prob > F value
Model	17	34301.18	2017.72	$2.902 \cdot 10^{8}$	0.0001
A	1	948.25	948.25	$1.364 \cdot 10^{8}$	0.0001
B	1	133.29	133.29	$1.917 \cdot 10^{7}$	0.0001
C	1	14265.11	14265.11	$2.052 \cdot 10^{9}$	0.0001
D	1	18109.27	18109.27	$2.605 \cdot 10^{9}$	0.0001
E	1	10.87	10.87	$1.563 \cdot 10^{6}$	0.0001
F	1	29.97	29.97	$4.311 \cdot 10^{6}$	0.0001
AB	1	46.16	46.16	$6.639 \cdot 10^{6}$	0.0001
AC	1	548.40	548.40	$7.888 \cdot 10^{7}$	0.0001
AD	1	0.076	0.076	10928.71	0.0001
AE	1	$5.653 \cdot 10^{-4}$	$5.653 \cdot 10^{-4}$	81.30	0.0001
AF	1	0.45	0.45	64532.10	0.0001
BF	1	17.94	17.94	$2.581 \cdot 10^{6}$	0.0001
CF	1	121.62	121.62	$1.749 \cdot 10^{7}$	0.0001
DF	1	$1.156 \cdot 10^{-4}$	$1.156 \cdot 10^{-4}$	16.62	0.0002
EF	1	$3.511 \cdot 10^{-5}$	$3.511 \cdot 10^{-5}$	5.05	0.0295
ABF	1	14.99	14.99	$2.156 \cdot 10^{6}$	0.0001
ACF	1	54.78	54.78	$7.879 \cdot 10^{6}$	0.0001
Error	46	$3.198 \cdot 10^{-4}$	$6.953 \cdot 10^{-6}$		
$R^2 = 0.99$					

A regression analysis using the least-squares estimation method on the values of the response obtained from the various combinations of the factors yields the following two equations (5.1 and 5.2) for the total energy consumption in case of no channel errors and with channel errors, respectively.

$$
\begin{aligned}
Total_{Energy} = {} & +105.08 + 2.15A + 2.29B + 11.94C + 16.86D + 0.41E - 0.15F \\
& + 1.02AF + 1.0BF - 2.25CF
\end{aligned}
\tag{5.1}
$$

$$
\begin{aligned}
Total_{Energy} = {} & +111.26 - 3.85A + 1.44B + 14.93C + 16.82D + 0.41E + 0.68F \\
& + 0.85AB - 2.93AC + 0.034AD + 2.97 \cdot 10^{-3}AE + 0.084AF + 0.53BF \\
& - 1.38CF - 1.34 \cdot 10^{-3}DF - 7.41 \cdot 10^{-4}EF + 0.48ABF - 0.93ACF
\end{aligned}
\tag{5.2}
$$

Figures 5.1(a), 5.1(b), and 5.2 show the three-dimensional response surface graphs with corresponding contour plots for the total energy consumption obtained from the regression models for packet size and the Tx and Rx factors. Notice that because the model contains interaction between the packet size and Tx and Rx, the contour line of total energy consumption are curved.

Furthermore, table 5.2 shows that the energy consumption of the listening factor in case of channel errors is higher than the one in case of no channel errors (see Table 5.1). The reason is due to the energy spending for retransmission. Similar to the listening factor, the transmit energy is much higher in case of channel errors due to the retransmission of lost packets as well as the NACK from the receiver.

(a) Packet size vs. Tx
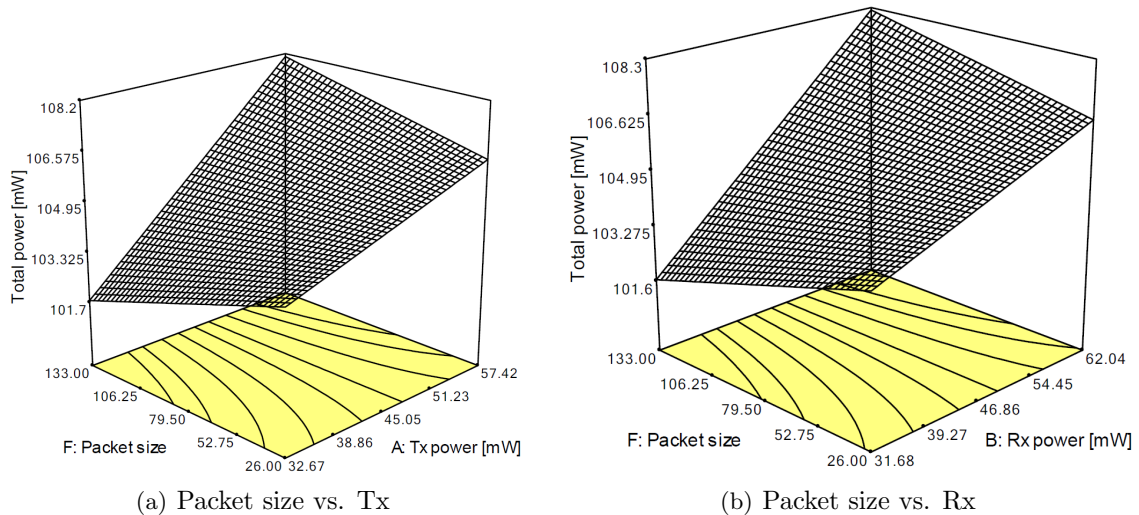

(b) Packet size vs. Rx

Figure 5.1: The response surface graph of total energy consumption in case of no channel errors
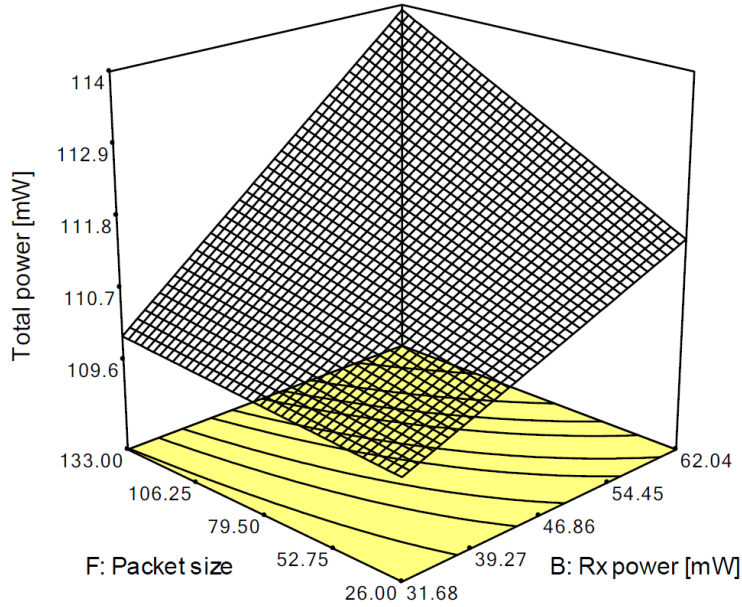
Figure 5.2: The response surface graph of total energy consumption in case of channel errors for Rx packet size factors

5.2 Results in case of a random topology

Tables 5.5 and 5.7 show the percentage of the individual factors and, their pairwise combinations contribute to the total energy consumption in case of no channel errors and with channel errors, respectively.

Similar to the previous results we show the analysis of variance (ANOVA) in Tables 5.6 and 5.8.

A regression analysis using the least-squares estimation method on the values of the response obtained from the various combinations of the factors yields the following two equations (5.3 and 5.4) for the total energy consumption in case of no channel errors and with channel errors, respectively.

In short, we can conclude that despite the underlying different network topology, our regression analysis are fairly stable. Please compare equations (5.3 and 5.4) with equations (5.1 and 5.2)

$$
\begin{aligned}
Total_{Energy} = {} & +107.60 + 2.18A + 2.32B + 12.70C + 16.84D + 0.43E \\
& - 0.15F + 1.02AF + 1.0BF - 2.25CF
\end{aligned} \tag{5.3}
$$

$$
\begin{aligned}
Total_{Energy} = {} & +113.91 - 3.93A + 1.48B + 15.70C + 16.80D + 0.43E + 0.54F \\
& + 0.84AB - 2.93AC + 0.035AD + 2.516 \cdot 10^{-3}AE + 0.23AF + 0.54BF \\
& - 1.44CF - 2.656 \cdot 10^{-4}DF - 8.438 \cdot 10^{-4}EF + 0.48ABF - 0.86ACF
\end{aligned} \tag{5.4}
$$

Table 5.5: The percentage of factors contribution in case of no channel errors: random topology

Term	Sum of Squares	Percentage contribution
A	305.203	1.032
B	343.229	1.160
C	**10323.3**	**34.893**
D	**18145.4**	**61.332**
E	11.687	0.040
F	1.431	$4.838 \cdot 10^{-3}$
AF	66.546	0.225
BF	64.087	0.217
CF	324.43	1.096
Error	0	

Table 5.6: ANOVA for total energy consumption in case of no channel errors: random topology

Source	Degree of freedom	Sum of squares	Mean Square	F-value	Prob > F value
Model	9	29585.32	3287.26	$6.366 \cdot 10^7$	0.0001
A	1	305.20	305.20	$6.366 \cdot 10^7$	0.0001
B	1	343.23	343.23	$6.366 \cdot 10^7$	0.0001
C	1	10323.28	10323.28	$6.366 \cdot 10^7$	0.0001
D	1	18145.42	18145.42	$6.366 \cdot 10^7$	0.0001
E	1	11.69	11.69	$6.366 \cdot 10^7$	0.0001
F	1	1.43	1.43	$6.366 \cdot 10^7$	0.0001
AF	1	66.55	66.55	$6.366 \cdot 10^7$	0.0001
BF	1	64.09	64.09	$6.366 \cdot 10^7$	0.0001
CF	1	324.43	324.43	$6.366 \cdot 10^7$	0.0001
Error	54	0.000	0.000		
$R^2 = 0.99$					

Table 5.7: The percentage of factors contribution in case of channel errors: random topology

Term	Sum of Squares	Percentage contribution
A	988.081	2.759
B	139.393	0.389
C	**15776.9**	**44.053**
D	**18066.7**	**50.447**
E	11.5881	0.032
F	18.880	0.052
AB	45.037	0.126
AC	549.785	1.535
AD	0.079	$2.205 \cdot 10^{-4}$
AE	$4.05 \cdot 10^{-4}$	$1.131 \cdot 10^{-6}$
AF	3.3	$9.207 \cdot 10^{-3}$
BF	18.555	0.052
CF	132.736	0.371
DF	$4.51563 \cdot 10^{-6}$	$1.261 \cdot 10^{-8}$
EF	$4.55625 \cdot 10^{-5}$	$1.272 \cdot 10^{-7}$
ABF	14.515	0.040
ACF	47.764	0.133
Error	$1.202 \cdot 10^{-4}$	

Table 5.8: ANOVA for total energy consumption in case of channel errors: random topology

| Source	Degree of freedom	Sum of squares	Mean Square	F-value	Prob > F value
Model	17	35813.30	2106.66	$8.064 \cdot 10^8$	0.0001
A	1	988.08	988.08	$3.782 \cdot 10^8$	0.0001
B	1	139.39	1139.39	$5.336 \cdot 10^7$	0.0001
C	1	15776.93	15776.93	$6.039 \cdot 10^9$	0.0001
D	1	18066.65	18066.65	$6.916 \cdot 10^9$	0.0001
E	1	11.59	11.59	$4.436 \cdot 10^6$	0.0001
F	1	18.88	18.88	$7.227 \cdot 10^6$	0.0001
AB	1	45.04	45.04	$1.724 \cdot 10^7$	0.0001
AC	1	549.79	549.79	$2.104 \cdot 10^8$	0.0001
AD	1	0.079	0.079	30225.09	0.0001
AE	1	$4.050 \cdot 10^{-4}$	$4.050 \cdot 10^{-4}$	155.03	0.0001
AF	1	3.30	3.30	$1.26 \cdot 10^6$	0.0001
BF	1	18.56	18.56	$7.103 \cdot 10^6$	0.0001
CF	1	132.74	132.74	$5.081 \cdot 10^7$	0.0001
DF	1	$4.516 \cdot 10^{-6}$	$4.516 \cdot 10^{-6}$	1.73	0.1951
EF	1	$4.556 \cdot 10^{-5}$	$4.556 \cdot 10^{-5}$	17.44	0.0001
ABF	1	14.52	14.52	$5.556 \cdot 10^6$	0.0001
ACF	1	47.76	47.76	$1.828 \cdot 10^7$	0.0001
Error	46	$1.202 \cdot 10^{-4}$	$2.612 \cdot 10^{-6}$		
$R^2 = 0.99$					

5.3 Discussion of the results

The results of the total energy consumption in WHART TDMA system can be explained as follows. In TDMA systems nodes can spend much of their time in sleep state. When sleeping, a node consumes a small amount of energy that is accumulated over the lifetime of the node. In the WHART TDMA protocol a node wakes up at the beginning of a time slot it is involved in and spends a certain amount of time in the listen state – TxRxOffset when it is a receive slot and TxTxOffset when it is a transmit slot. Furthermore, for each transaction a transmitting node has to switch to the listening state for a duration of RxWait (about 2.2ms) and for RxAckWait (about 1ms) for listening for acknowledgments from other devices in the network. In addition, each node spends additional time on each single transaction for switching the channel, and for listening to the channel to enable the joining of new nodes, and the other control packets such as keep-alive and maintenance packets (every 60 sec) in the network, thereby contributing to the additional energy consumption in the network. Additionally, based on the hop count of the node from the gateway, the listening time of the node varies, a node near to the gateway listens more compared to the source. Thus, in WHART TDMA, the listening time is a major factor for energy consumption. Listening consumes more energy than transmission and reception. Thus, by optimizing this listening time (within the constraints given by synchronization accuracy, packet size, resynchronization and maintenance packets) the energy consumption can be reduced significantly.

TKN-11-001
Page 28

5.4 Impact of synchronization on the energy consumption

In order to study the impact of time synchronization and the associated control packets (keep-alive, join/request/response and health report packets) on the total energy consumption, we compare the same setup as described in Section 4.1 with and without running the synchronization protocol for both single and multiple scenarios.

5.4.1 Single-flow scenario
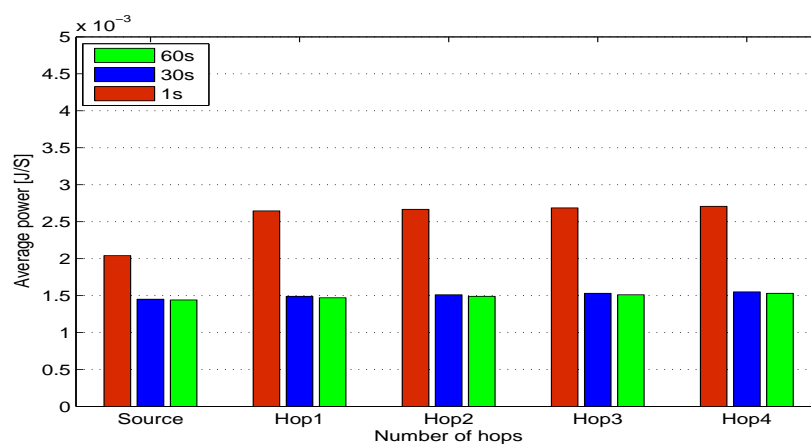
(a) Without synchronization control packets
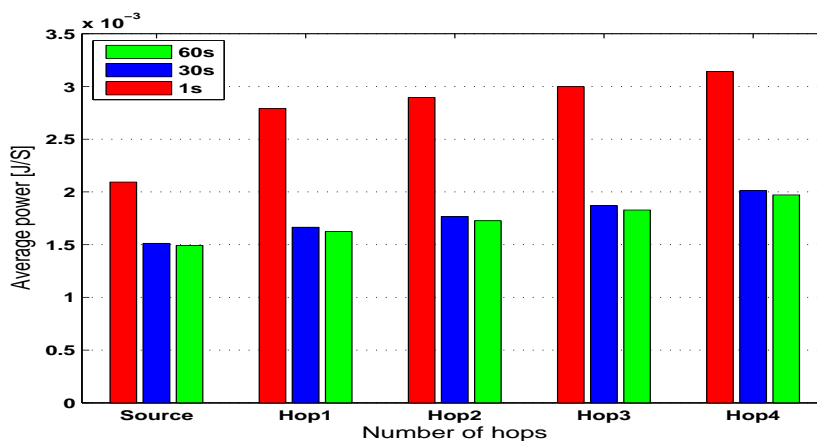
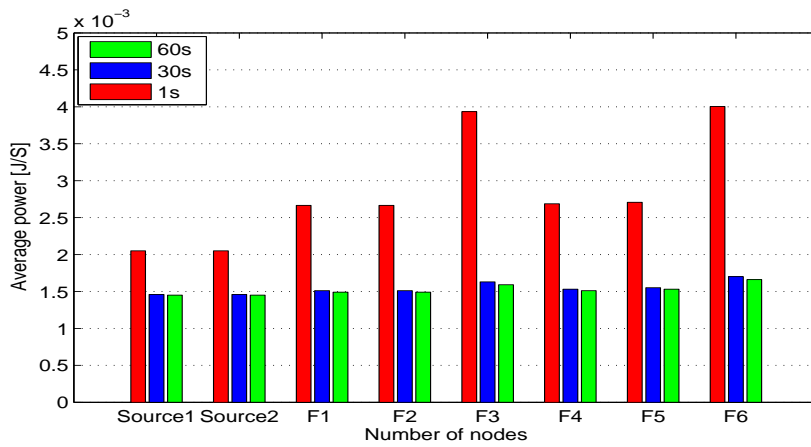

(b) With synchronization control packets

Figure 5.3: Energy consumption in case of single flow scenario

Figures 5.3(a) and 5.3(b) show the energy consumption of each node with respect to the data scan rate with/without synchronization, respectively. The data scan rate is varied by changing the sensor report interval time on the source node by 1, 30, and 60 seconds. As can be seen from Figure 5.3(a) that all the forwarder nodes have approximately the same energy

consumption with respect to hop number. The energy consumption in case of synchronized network shown in Figure 5.3(b), is higher as the node gets closer to the gateway due to the control packets that are forwarded to the gateway from all the nodes.

5.4.2 Multiple-flow scenario

Figures 5.4(a) and 5.4(b) show the energy consumption of each node in case of multiple path scenario with respect to the data scan rate with/without synchronization respectively. The energy consumption shown in Figure 5.4(a) is approximately the same for all the forwarders, except in F3 and F6, since they share multiple incoming flows.

(a) Without synchronization control packets
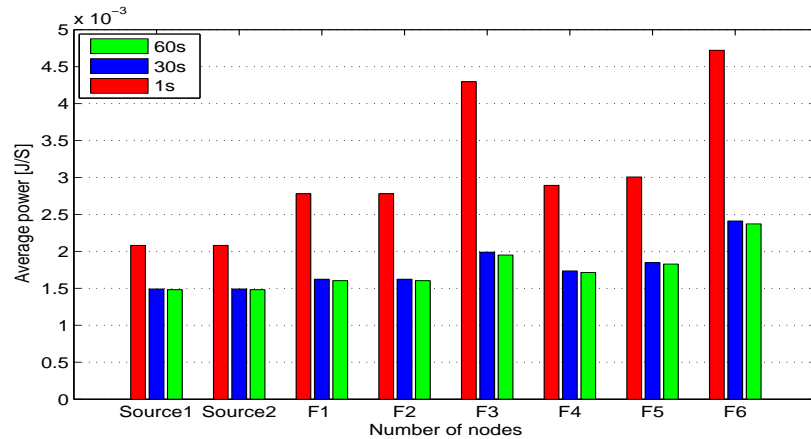
(b) With synchronization control packets

Figure 5.4: Energy consumption in case of multiple flow scenario

he energy consumption at the forwarder nodes near the GW varied based on the a mount of control packets received/forwarder to other nodes.

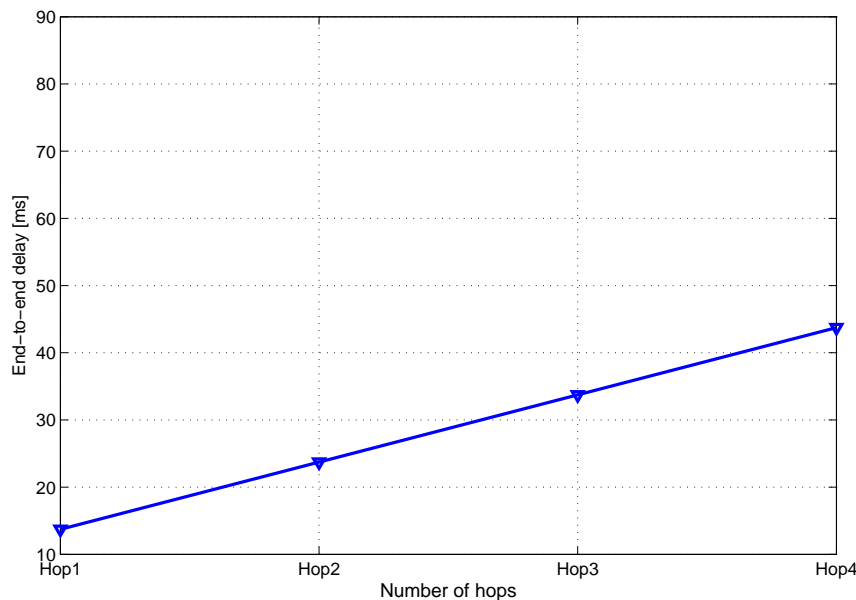Therefore the forwarder at F6 (Figure 5.4(b)) has higher energy consumption compared

Figure 5.5: Single flow scenario, end-to-end delay

to forwarder at F3 as it received more number of control packets than forwarder at F3. Please note that F6 and F3 share the same number of flows. Moreover, figures 5.3(a), 5.3(b), 5.4(a) and 5.4(b) show that the energy consumption for the scenario with the highest packet sampling rate (1s) has the highest energy consumption. The energy consumption for the scenario with 60s sampling rate is close to the one with 30s sampling rate, this is due to the sleeping energy as most of the time the nodes are sleeping.

5.5 Impact of type of scheduler algorithms on the end-to-end delay

In this section we discuss the results of end-to-end delay observed by an individual node and gateway when operated under a particular link scheduler.

5.5.1 Single-flow scenario

Similar to other TDMA protocols, WirelessHART TDMA has bounded delay due to the deterministic and centralized scheduling. Figure 5.5 shows that the end-to-end delay is linear with the number of hops.
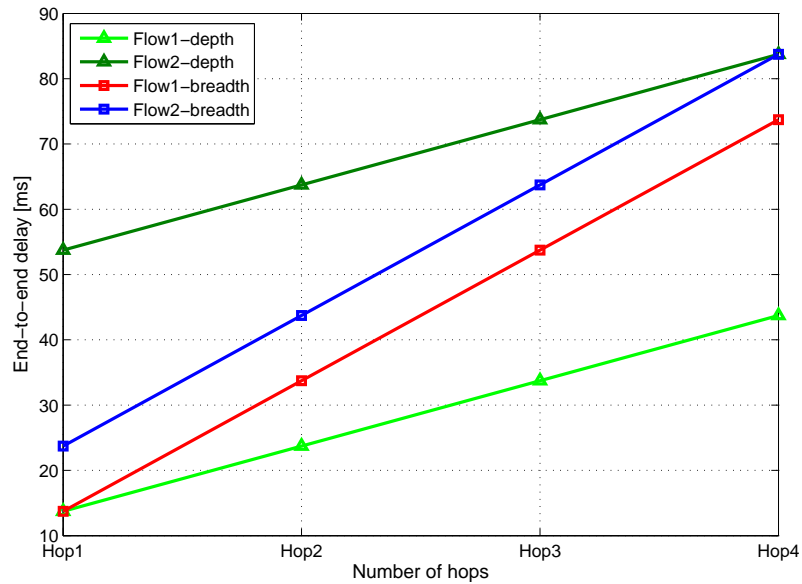
Figure 5.6: Multiple flow scenario, end-to-end delay

5.5.2 Multiple-flow scenario

In breadth-based scheduling slots are assigned sequentially based on the hop number of the nodes. Therefore the multiple flows have closer end-to-end delay compared to depth-based scheduling. As can be seen in Figure 5.6 the difference in end-to-end delay for depth-based scheduling is quite higher than breadth-based scheduling.

Chapter 6

Related work

In this section, we present the related work in the area of the low-power MAC protocols and distributed operations for multi-hop wireless mesh networks. One of the main concerns of low-power MAC protocols is to switch the radio into sleep mode as much as possible, otherwise energy would be wasted. The main factor contributing to the energy dissipation is the idle listening (nodes that waiting for potential incoming traffics). Other factors that also contribute to such wastage are: collision, overhearing, control packets such as clock synchronization and maintenance packets, and other protocol overheads. Such MAC protocols may be broadly classified into three main categories: random-based, slotted-based and scheduled-based. In the random-based access called low-power listening (LPL) such as B-MAC [20], WiseMAC [6]. There is no need to coordinate the cycles and therefore there is not need of clock synchronization. Each node periodically wakes up and checks the channel activity for short time without receiving any data. If the channel is idle it goes sleep otherwise, it stays awake to receive the packet. To rendezvous with receivers, senders send a long preamble before each message (longer than the checking interval).

In the slotted-based access such as S-MAC [28] and T-MAC [25], nodes required to be synchronized and time is organized into equal slots size. Each slot divided into two time intervals. In the first time interval nodes can exchange synchronization information. In the second interval node may receive or send based on the RTS-CTC. A general problem shared by all such slotted-based protocols is that communication is grouped at the beginning of each slot, raising the chances on collisions, hence limiting their dynamic range to low traffic rates only.

Our work related to the scheduled-based access (TDMA). TDMA protocols allocate an exclusive time slot for data transmissions between node pairs. In these protocols slot assignment algorithms and tight clock synchronization algorithms are of a great concern. LMAC [26] uses a simple random slot assignment algorithm that ensures that nodes at 2-hop distance do not use the same slot number. It assumes a global time synchronization. Similar to the LMAC, TRAMA [21] uses distributed election scheme to determine particular time slots, however it uses more complicated polices that take traffic load into account which induce extra complicity and relatively large memory for maintaining scheduling information among neighbors. A state-of-the-art solution for a TDMA based system is the WirelessHART standard as explained in section 2, uses centralized scheduling mechanism. To the best of our knowledge, this is the first attempt of implementing and evaluating WirelessHART TDMA

protocol. We also identify the factors contributing most to the overall network energy consumption, thus we provide guidance on where to start with any effort geared towards saving energy.

Chapter 7

Conclusions and future research

A state-of-the-art solution for TDMA based system is the WirelessHART standard. WirelessHART is one of the first wireless communication standards specifically designed for process automation applications. The standard has been finalized in 2007, and at the beginning of 2010 it has been ratified as an IEC standard. Throughout this report a performance evaluation of WHART TDMA has been presented. Namely, we presented the following main contributions:

(1) We implemented WirelessHART TDMA protocol using Castalia and OMNeT++ simulation framework. (2) We performed a sensitivity analysis using response surface methodology to obtain some insights on how the overall energy consumption breaks down into different factors (Tx , Rx, Listen, Sleep, turnover, and packet size). By identifying the factors contributing most to the overall network energy consumption, we provided guidance on where to start with any effort geared towards saving energy. We obtain a regression models for total energy consumption under different scenarios. These regression models provide a clear break down of the major components influencing most to the energy consumption in the WirelessHART. We discussed why the sleeping and listening times are the major factors contributing to the energy consumptions in the WirelessHART TDMA system. To the best of our knowledge, this is the first attempt of providing a clear break down of the major components, which contribute to the energy consumption.

(3) We also evaluated and discussed the impact of synchronization on the performance of WirelessHART TDMA protocol.

Future work will focus on the improvement of WHART TDMA protocol, namely to study optimizations that minimize the total energy consumption of the time slots taking into account WHART constrains such as synchronization accuracy, and management packets rates. Further work will also continue to investigate the impact of the routing and link scheduling parameters to the total energy consumption model. Please note that our study assumes that the behaviours of all the channels are exactly the same as a single channel behaviour. We only model the energy switching cost among the channels. Thus we intend to enhance the current channel model by adding hopping mechanism with (e.g. fading model) among different channels.

Bibliography

[1] *ISA 100: wireless system for automation. Available: http:// isa.zigbee.org.*

[2] *ZigBee Alliance. Available: http:// www.zigbee.org.*

[3] M. Adler, R. K. Sitaraman, A. L. Rosenberg, and W. Unger. Scheduling time-constrained communication in linear networks 1998, pp. 269 278. In *Proc. ACM Symposium on Parallel Algorithms and Architectures (SPAA)*, 1998.

[4] Chipcon. *CC2420 2.4 GHz IEEE 802.15.4 / ZigBee-ready RF Transceiver Available: http://www.chipcon.com.*, 2004.

[5] Dust Networks. *Wirelesshart technical data sheet. White paper, Dust Networks, September 2007.*

[6] A. El-Hoiydi, J.-D. Decotignie, C. Enz, and E. Le Roux. Poster abstract: Wisemac, an ultra low power mac protocol for the wisenet wireless sensor network. In *Proc. ACM SenSys 03*, Los Angeles, California, November 2003. Poster Abstract.

[7] Jeremy Elson and Deborah Estrin. Random, ephemeral transaction identifiers in dynamic sensor networks. In *Proc. 21st International Conference on Distributed Computing Systems (ICDCS-21)*, April 2001.

[8] Jeremy Elson and Kay Romer. Wireless sensor networks: A new regime for time synchronization. In *Proc. HotNets-I First Workshop on Hot Topics In Networks*, New Jersey, USA, October 28-29 2002.

[9] Steven D. Glaser. Some real-world applications of wireless sensor nodes. In *Proc. (SPIE) Symposium on Smart Structures and Materials/ NDE 2004*, San Diego, California, March 2004.

[10] HART Communication Foundation. *HART Communication Protocol Specification, HCF SPEC 13 Revision 7.1, 05 June, 2008.*

[11] HART Communication Foundation. *Network Management Specification, HCF SPEC 085 Revision 1.1, 30 May, 2008.*

[12] HART Communication Foundation. *TDMA Data Link Layer Specification, HCF SPEC 075 Revision 1.1, 17 May, 2008.*

[13] HART Communication Foundation. *WirelessHART Device Specification, HCF SPEC 290 Revision 1.1, 22 May, 2008.*

[14] Koen Langendoen. Medium access control in wireless sensor networks. In H. Wu and Y. Pan, editors, *Medium Access Control in Wireless Networks.* Nova Science Publishers, May 2008.

[15] LAN/MAN Standards Committee of the IEEE Computer Society. *IEEE STD 802.15.4-2006. Wireless Medium Access Contril (MAC) and Physical Layer (PHY) Specifications for Low-Rate Wireless Personal Area Networks (WPANs) Task Group. Available: http://www.ieee802.org/15/pub/TG4.html*, 2006.

[16] B. Krishnamachari M. Zuniga. Analyzing the transitional region in low power wireless links. In *First IEEE International Conference on Sensor and Ad hoc Communications and Networks (SECON)*, Santa Clara, CA,, October 2004.

[17] R.H. Myers and D.C. Montgomery. *Response Surface Methodology.* John Wiley and Sons,Inc, 2002.

[18] Suman Nath, Phillip B. Gibbons, Srinivasan Seshan, and Zachary Anderson. Synopsis diffusion for robust aggregation in sensor networks. In *Proc. ACM Transactions on Sensor Networks, 2008*, volume vol.2, March 2008.

[19] NICTA. *The Castalia simulator for Wireless Sensor Networks. Available: http://castalia.npc.nicta.com.au.*

[20] Joseph Polastre, Jason Hill, and David Culler. Versatile low power media access for wireless sensor networks. In *Proc. 2nd international conference on Embedded networked sensor systems (ACM SenSys)*, Baltimore, MD, November 2004.

[21] Venkatesh Rajendran, Katia Obraczka, and J. J. Garcia-Luna-Aceves. Energy-efficient, collision-free medium access control for wireless sensor networks. In *Proc. ACM SenSys 03*, Los Angeles, California, November 2003.

[22] Reuven Y. Rubinstein and Benjamin Melamed. *Modern Simulation and Modeling.* Wiley Interscience, New York, 1998.

[23] Robert Szewczyk, Alan Mainwaring, Joseph Polastre, John Anderson, and David Culler. An analysis of a large scale habitat monitoring application. In *Proc. ASM SenSys '04*, pages 214–226, 2004.

[24] Gilman Tolle, Joseph Polastre, Robert Szewczyk, David Culler, Neil Turner, Kevin Tu, Stephen Burgess, Todd Dawson, Phil Buonadonna, David Gay, and Wei Hong. A macroscope in the redwoods. In *Proc. ACM SenSys '05*, pages 51–63, 2005.

[25] T. van and D. K. Langendoen. An adaptive energy-efficient mac protocol for wireless sensor networks. In *Proc. ACM SenSys '03'*, Los Angeles, California, USA., November. 2003.

[26] L.F.W. van Hoesel and P.J.M. Havinga. A lightweight medium access protocol for wireless sensor networks. In *Proc. INSS, 2004*, 2004.

[27] A. Varga. *OMNeT++ Discrete Event Simulation System.* Available: *http://www.omnetpp.org.*

[28] Wei Ye, John Heidemann, and Deborah Estrin. An energy-efficient mac protocol for wireless sensor networks. In *Proc. INFOCOM 2002*, New York, June 2002. IEEE.